International Journal of Economy, Energy and Environment
2023; 8(5): 104-112
http://www.sciencepublishinggroup.com/j/ijeee
doi: 10.11648/j.ijeee.20230805.11
ISSN: 2575-5013 (Print); ISSN: 2575-5021 (Online)

Comparisons of the Added Value of Dynamical Downscaling of ECMWF EPS and NCEP GEFS for Wind Forecast in the Complex Terrain of Sichuan and Yunnan in China

Zifen Han[1], Bolin Zhang[1], Jianmei Zhang[2], Jie Long[1], Xiaohui Zhong[3, *]

[1]State Grid Gansu Electric Power Company, Lanzhou, China

[2]School of Information Science and Engineering, Lanzhou University, Lanzhou, China

[3]Envision Digital International Pte Ltd, Singapore

Email address:

x7zhong@gmail.com (Xiaohui Zhong)

[*]Corresponding author

To cite this article:

Zifen Han, Bolin Zhang, Jianmei Zhang, Jie Long, Xiaohui Zhong. Comparisons of the Added Value of Dynamical Downscaling of ECMWF EPS and NCEP GEFS for Wind Forecast in the Complex Terrain of Sichuan and Yunnan in China. *International Journal of Economy, Energy and Environment*. Vol. 8, No. 5, 2023, pp. 104-112. doi: 10.11648/j.ijeee.20230805.11

Received: September 15, 2023; **Accepted**: October 24, 2023; **Published**: October 28, 2023

Abstract: Numerical weather prediction (NWP) models are commonly used for wind power forecasts, but NWP forecasts are uncertain due to uncertainties in the initial conditions, approximate model physics, and the chaotic nature of the atmosphere. Ensemble prediction systems (EPS), which simulate multiple possible futures, thus provide valuable information about forecast uncertainties. However, the spatial resolution of global ensemble forecasts from the European Centre for Medium-range Weather Forecast (ECMWF) and the National Centers for Environmental Prediction (NCEP) is relatively coarse and insufficient for many wind power farms built in complex terrain. This work proposes using the Weather and Research Forecasting model (WRF) to downscale ECMWF EPS and NCEP global ensemble forecast system (GEFS) to determine and compare the added values of downscaling different global EPS forecasts for wind forecasts in the complex terrain of Sichuan and Yunnan in China. A total of 366 days of day-ahead forecasts (28 to 51 hours) for wind speed at 80 meters are evaluated. The results demonstrate that the ensemble average of the higher resolution WRF downscaled forecast is considerably better than that of the global EPS forecast, and downscaled forecast of ECMWF EPS achieves the best performance. Also, a selective ensemble average (SEA) method is proposed and applied for the ultra-short (10 to 13 hours) forecast. Verification results demonstrate that the SEA method outperforms the ensemble mean.

Keywords: Wind Forecast, Ensemble, WRF, Downscaling

1. Introduction

At the end of 2022, China had about 365 GW of wind generation capacity installed, according to data from China's National Energy Administration (NEA). In 2022, wind power plants provided about 8% of China's electricity production and accounted for 10% of China's installed power generating capacity. Meanwhile, wind power prices have decreased and become comparable with coal-fired power generation [1, 2]. In 2011, China's NEA drafted a regulation requiring a 15-minute resolution of both a 24-hour ahead wind forecast (96 steps) and 4 hours ahead ultra-short wind forecast (16 steps) (Chinese GBT). In addition, penalties are imposed for wind farms that exceed the presupposed error threshold [3]. Due to regulation and the increasing wind power percentage of the energy mix of China and the world, the accurate wind power forecast is increasingly important for large-scale wind energy penetration [4, 5].

Numerical weather prediction (NWP) models are widely used for wind power forecasts [6, 7]. However, using NWP models for wind power forecasts suffers from several uncertainties. Firstly, the atmospheric system is chaotic, and minor errors in the initial conditions can grow dramatically [8, 9]. Such errors in the initial conditions of NWP models are inevitable due to insufficient observations, which affect NWP

forecast accuracy as NWP is essentially an initial value problem [10, 11]. Secondly, approximate simulations of the complex atmospheric processes cause errors limiting NWP's predictability [8]. Therefore, the ensemble prediction system (EPS) is often used for estimating forecast uncertainty [12]. In the early 1990s, both the European Centre for Medium-range Weather Forecast (ECMWF) and the National Centers for Environmental Prediction (NCEP) Toth et al. developed their operational EPS [13-17]. Currently, the ECMWF EPS uses 18 km horizontal resolution and 91 vertical levels and contains one control member and 50 perturbed members [18]. On the other hand, the NCEP global ensemble forecast system (GEFS) uses 34 km horizontal resolution and 64 vertical levels with one control member and 20 perturbed members [19].

Since many wind power plants are built in complex terrain, higher than the coarse resolution of global EPS data is needed to resolve topographic impact and local patterns. Dynamical downscaling using a mesoscale NWP model is one of the most common approaches to obtaining higher spatial resolution. Horvath et al. applied Aire Limitée Adaption dynamique Développement International (ALADIN) model to downscale the ECMWF reanalysis (ERA-50) data to 8 km horizontal grid spacing in the complex terrain of Croatia for ten years [20]. The statistical verification against wind speed measurement suggested that the downscaling improved the model accuracy. Marjanovic et al. ran the Weather Research and Forecasting (WRF) model to downscale the North American Regional Reanalysis (NARR) data for wind farms located in the complex terrain on the West Coast of the United States [21]. They compared WRF predicted wind speed of different resolutions and showed significant improvement of higher resolution simulations compared to lower resolution simulations, especially during weak forcing. Jiménez and Dudhia proposed a new parameterization to account for the effects of the unresolved topography that exerts over the surface circulation in WRF [22]. Their results demonstrated that the WRF simulation using the new scheme outperforms the default WRF simulation regarding surface wind over the complex terrain region located northeast of the Iberian Peninsula.

Dynamical downscaling of the global ensemble is also applied for constructing regional EPS (REPS) with initial conditions and lateral boundary conditions provided by ensemble members of global EPS [23]. Branković et al. used the ALADIN-Limited Area Ensemble Forecasting (ALADIN-LAEF) model to downscale ECMWF EPS over the central European and northern Mediterranean domain for four severe weather cases [24]. The verification result indicated that the downscaled ensemble of higher resolution improves the precipitation rate and pattern. Weidle et al. also used the ALADIN-LAEF model to downscale ECMWF EPS and NCEP GEFS for 51 days in the 2010 summertime over central Europe [23]. The comparisons revealed that using GEFS performs better for surface parameters, while using EPS is superior at upper levels. Zhang et al. constructed the operational REPS of North China using the WRF model to downscale GEFS to forecast severe local weather [25]. They illustrated that the downscaling improves ensemble verification scores.

The dynamical downscaling of the global ensemble has been successfully applied in several REPS for many years, and the REPS is also used for building operational wind forecast systems thanks to increasing computational resources. The WRF model is extensively implemented for downscaling global operational forecast data of coarse resolution [26, 27]. The aim of this work is to downscale both ECMWF EPS and NCEP GEFS using the WRF model and evaluate the potential benefits of downscaling global EPS forecast for operational wind forecast complex terrain wind farms in Sichuan and Yunnan, China. The effects of downscaling are evaluated by comparing the ensemble mean of the day-ahead and ultra-short forecast from the high-resolution WRF model with the global ensemble.

The ensemble mean is the average of all the ensemble members, but it is not necessarily the best way to use the ensemble forecasts [28]. Qi et al. assumed that the ensemble member performing well at the short lead time would also have smaller errors at the long lead time [29]. Thus, they proposed a methodology to select the ensemble members of which 0-12 hour forecast error is smaller than the ensemble mean (called SEA_Qi). The ensemble average of selected members is shown to have better skill than the ensemble mean of all members for 24, 48, 72, and 120 hours tropical cyclone track forecast. Kikuchi et al. compared different ensemble weighted-average methods for wind nowcasting and concluded that the SEA_Qi method performs better than the ensemble mean [30]. In light of these successful applications, we propose a selective ensemble average (SEA) method using wind turbine observation data for ultra-short-term wind forecasts. The proposed SEA method is also compared.

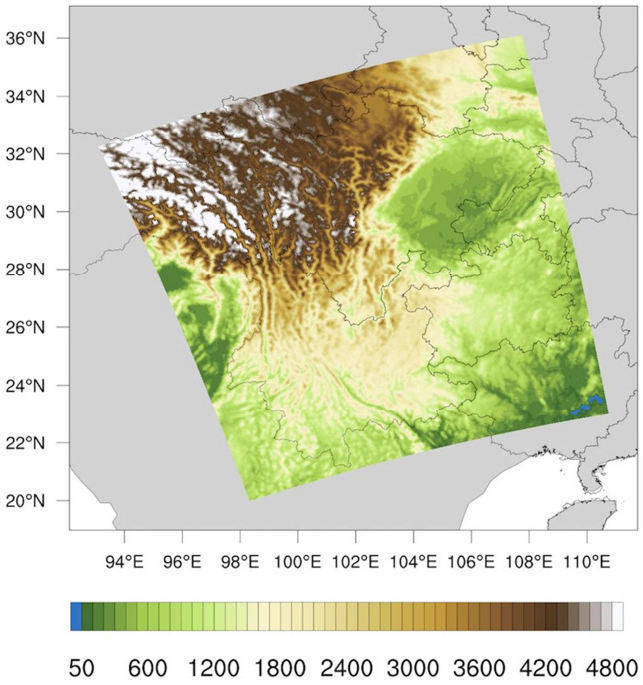

Figure 1. *Digital elevation data of the single WRF domain at a horizontal resolution of 5km. Black dots indicate the locations of wind farms.*

2. Data and Methods

2.1. WRF Model Configurations and Sea Method

2.1.1. WRF Model Configurations

We used the WRF model version 3.9.1 with initial and boundary conditions provided by the ensemble members of ECMWF EPS and the NCEP GEFS. As shown in Figure 1, the WRF model was configured with one single domain at a horizontal grid spacing of 5 km with 65 vertical levels. The WRF model performance largely depends on the choice of WRF scheme combinations. In order to find the best performing WRF configurations, we tested 79 combinations of planetary boundary layer (PBL) schemes, land surface models (LSM), and surface layer schemes, as we found that wind speed forecast is mostly sensitive to the PBL and LSM schemes. Similar to the methodology described by Huva et al., the WRF physics parameterizations were tested on a representative 15-day period [31]. The 15 days were selected based on daily average wind speed values throughout the year to cover all possible scenarios. As a result, the schemes selected include WRF Single-Moment 6-Class for microphysics, NCEP GFS scheme for PBL mixing, Pleim-Xiu LSM, Kain-Fritsch scheme for cumulus, and New Goddard for both longwave and shortwave radiation [32-37].

The WRF forecasts were run for 52 hours from each 1200 UTC release by downscaling all 51 members of EPS (WRF EPS) and 21 members of GEFS (WRF GEFS). Consistent with operational wind speed and power forecast required by 3, the day-ahead hours of 28 to 51 hours and ultra-short term of 10 to 13 hours were chosen for performance evaluation (Table 1).

Table 1. *Specification of forecast data.*

Ensemble forecast	Horizontal resolution	Number of ensemble members	Initial time (UTC)	Used day ahead forecast (hour)	Used ultra-short term forecast (hour)
Raw ECMWF HRES	0.1°	1	12	28 to 51	10 to 13
Raw NCEP GFS	0.25°	1			
Raw ECMWF EPS	0.2°	51			
Raw NCEP GEFS	0.5°	21			
WRF HRES	5km	1			
WRF GFS	5km	1			
WRF EPS	5km	51			
WRF GEFS	5km	21			

2.1.2. SEA Method

As discussed in Section 1, the ensemble average of selected members is possibly more accurate than the ensemble mean (of all members). This is because the members with smaller errors are selected based on past performance measured through observation data. Operationally, the global ensemble forecast product is available with a delay of a few hours after the initial time of forecast. The delay time is about 6 to 7 hours for NCEP GEFS and ECMWF EPS. Additionally, the wind power forecast providers, such as Envision, must make forecasts available for wind farms before 7 am Beijing Time, which allows at least 0 to 9 hours of forecasts to be evaluated by observations (because the forecast initial time of 12 UTC is 8 pm in Beijing Time).

The following steps calculate the SEA. Firstly, the root mean square error (RMSE, see Eq. 1) of the ensemble members' 0 to 9 hours wind forecast is calculated. Then, the ensemble members are ranked in descending order of their RMSE. Lastly, the average for top N (a hyper-parameter) members is calculated. Section 4 evaluates the impact of differences in N on ultra-short-term forecast performance. In addition, we follow 30 and add the average of the selected members with smaller than average RMSE (named SEA_Qi) in our evaluation.

2.2. Observation Data and Metrics for Evaluation

2.2.1. Observation Data

Each wind turbine has an anemometer installed on the nacelle behind the rotor at turbine hub height (i.e., 80 m above the surface). We utilize wind speed observations from 2 wind farms in Sichuan and 2 in Yunnan, China (black dots indicate the locations of wind farms in Figure 1). We compared the hourly observation data with NWP model output interpolated to 80 meters. The wind turbine observations represent a single local point in space, so we only extracted the nearest single point from the NWP domain.

In addition, we applied the following data quality control procedures to remove poor-quality observation data:

1. Remove data when either wind speed or wind power observation is missing.
2. Remove data when wind speed data is beyond the range of [0.0, 50.0] or wind power capacity factor (defined as actual power generated as a proportion of a wind turbine's maximum capacity) is beyond the range of [-0.1, 1.25].
3. Remove data of the same values that appear more than six times (observation is taken at the frequency of about 10 minutes) consecutively.

2.2.2. Evaluation Metrics

The study period covers the entire year of 2020, so 366 days of forecasts are used for evaluation in this work. Multiple metrics are used in this study to evaluate the performance of ensemble forecasts, including standard probabilistic verification scores: RMSE, mean bias error (MBE), and Pearson's correlation coefficient (CC) of the ensemble mean, as well as the continuous ranked probability score (CRPS) and rank histograms [38-40]. These measures are defined below:

$$RMSE = \sqrt{\sum(WS_{pred} - WS_{obs})^2/N} \quad (1)$$

$$MBE = \frac{1}{N}\sum(WS_{pred} - WS_{obs}) \quad (2)$$

where WSpred is the predicted wind speed WS, WSobs is the observed wind speed, and N is the number of pairs of forecast and observation.

The CRPS is calculated following:

$$CRPS = \sum_{-\infty}^{\infty}[F(y) - F_o(y)]^2 dy \quad (3)$$

$$F_o(y) = \begin{cases} 0, if\ y < observed\ value \\ 1, otherwise \end{cases} \quad (4)$$

Fo(y) is a cumulative probability step function that jumps from 0 to 1 when the forecast variable y equals the observations [41]. The CRPS generalizes the mean absolute error (MAE), and the smaller values of CRPS indicate better forecast skill. All the metrics were calculated at the 1-hour frequency.

In addition, the rank histogram allows a quick and straightforward demonstration of the qualities of the ensemble. A reliable EPS should have a flatter pattern [40]. A U-shape indicates a lack of spread (variability), while J or L-shapes indicate the presence of consistent biases.

3. Results and Discussion

3.1. Day Ahead Forecast and Ultra-Short Term Forecast Evaluation

Figures 2 and 3 illustrate the comparisons of the ensemble mean for the raw EPS, raw GEFS, WRF EPS, and WRF GEFS in terms of RMSE, MBE, CC, and CRPS over the four wind farms in the forecast lead time of day-ahead hours of 28 to 51 hours and ultra-short term of 10 to 13 hours, respectively. They clearly show that the ensemble mean of WRF EPS and WRF GEFS significantly outperforms the mean of the raw EPS and raw GEFS at all four wind farms, confirming the great benefits of downscaling global ensemble forecasts in complex terrain. Table 2 summarizes all the metrics averaged over the four wind farms. The forecast performance of WRF EPS is slightly better than WRF GEFS. However, the improvement of WRF downscaling is more dramatic for GEFS than EPS. The temporal evolution of wind speed RMSE, MBE, CC, and CRPS presented in Figure 4 demonstrates that WRF EPS is the most accurate forecast throughout all the forecast horizons. Figures 5 and 6 compare the rank histograms for all the ensembles in the four wind farms for both day-head and ultra-short-term forecasts, respectively. The rank histograms of raw EPS and GEFS for all farms are L-shaped and J-shaped, respectively, indicating significant negative and positive biases, consistent with MBE comparisons in Figures 2 and 3. Although the U- shaped rank histograms of WRF EPS and WRF GEFS also imply under-dispersed ensembles, they show many of the biases removed by WRF downscaling.

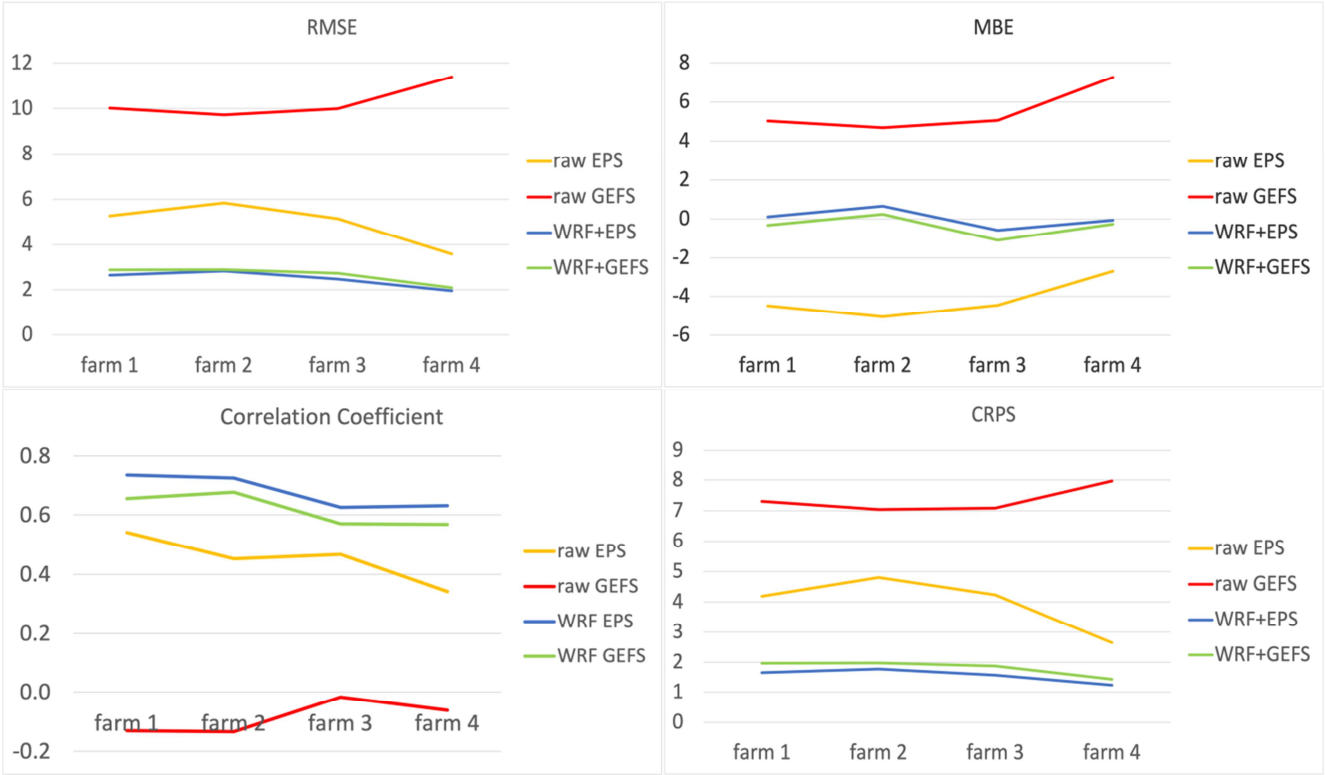

Figure 2. *28 to 51 hour wind forecast RMSE (top left), MBE (top right), and CC (bottom left) of ensemble mean of raw ECMWF EPS, raw NCEP GEFS, WRF EPS, and WRF GEFS for farm 1 and farm 2 in Sichuan and farm 3 and farm 4 in Yunnan as well CRPS (bottom right) for all the ensemble forecast.*

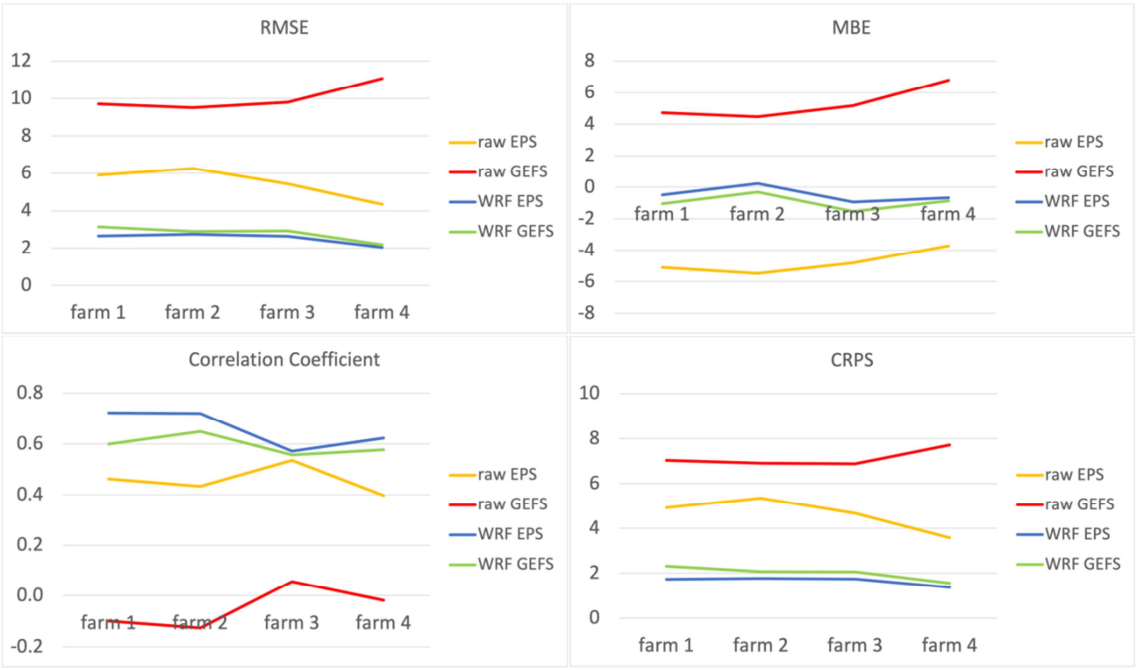

Figure 3. *10 to 13 hour wind forecast RMSE (top left), MBE (top right), and CC (bottom left) of ensemble mean of raw ECMWF EPS, raw NCEP GEFS, WRF EPS, and WRF GEFS for farm 1 and farm 2 in Sichuan and farm 3 and farm 4 in Yunnan as well CRPS (bottom right) for all the ensemble forecast.*

Table 2. *Summary of 28 to 51 hours and 10 to 13 hours wind speed forecast RMSE, MBE, CC, and CRPS average of all four wind farms for raw EPS, raw GEFS, WRF EPS, and WRF GEFS.*

	28 to 51 hours				**10 to 13 hours**			
	raw EPS	**raw GEFS**	**WRF EPS**	**WRF GEFS**	**raw EPS**	**raw GEFS**	**WRF EPS**	**WRF GEFS**
RMSE	5.26	10.13	2.60	2.74	5.72	9.89	2.60	2.86
MBE	-4.42	5.26	0.10	-0.28	-4.96	5.07	-0.35	-0.85
CC	0.44	-0.1	0.70	0.65	0.44	-0.06	0.69	0.62
CRPS	2.65	7.97	1.24	1.42	3.58	7.71	1.36	1.56

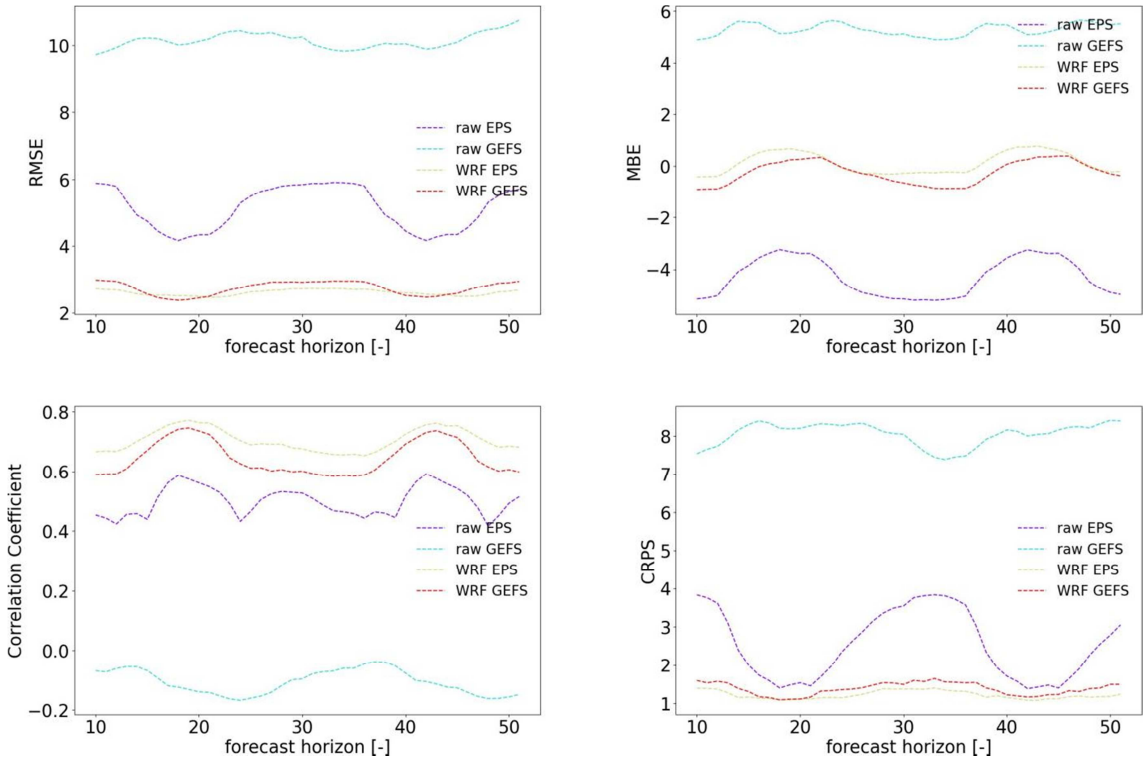

Figure 4. *RMSE, MBE, CC, and CRPS of ensemble mean of raw ECMWF EPS (top right), raw NCEP GEFS (top left), WRF EPS (bottom left), and WRF GEFS (bottom right) as function of forecast horizon from 10 to 51 hour wind forecast for 4 wind farms.*

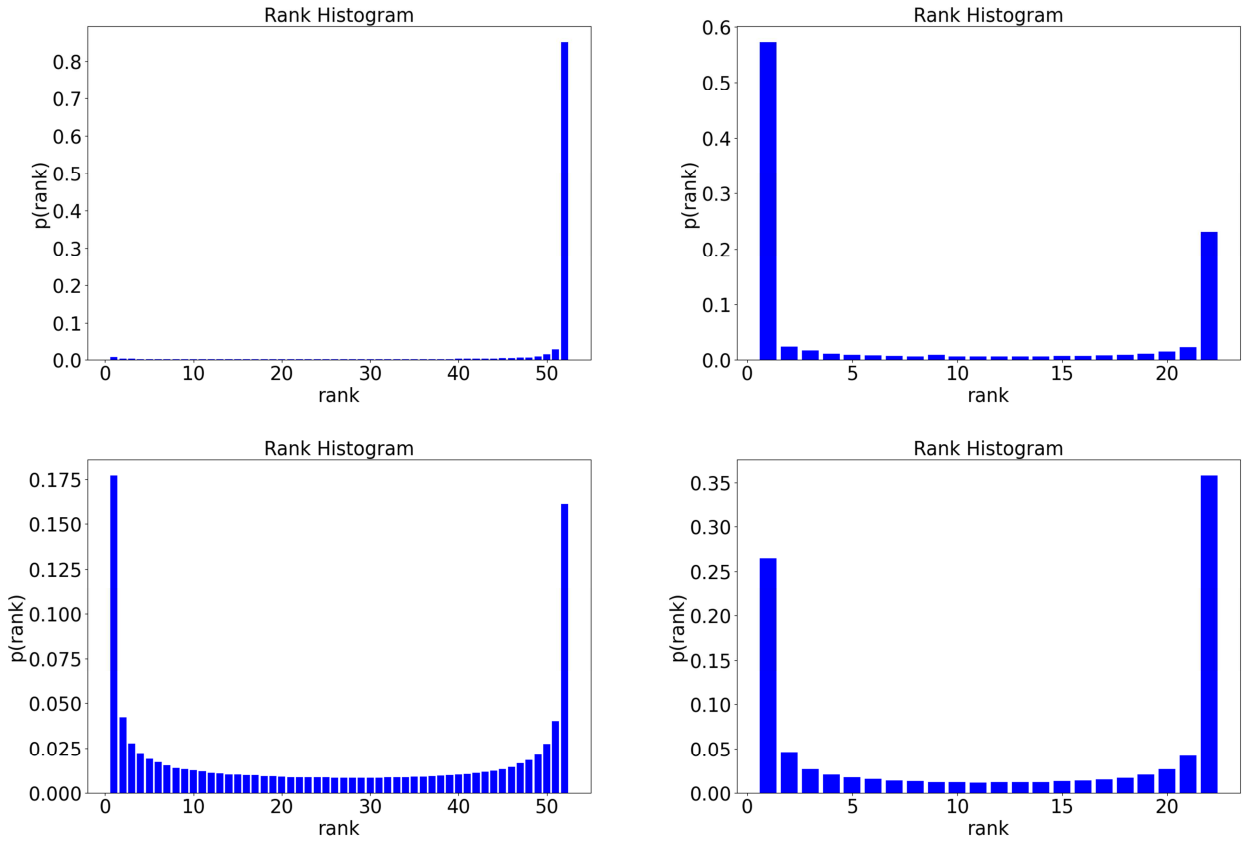

Figure 5. *Rank histograms of 28 to 51 hour wind forecast of raw ECMWF EPS (top right), raw NCEP GEFS (top left), WRF EPS (bottom left), and WRF GEFS (bottom right) for 4 wind farms.*

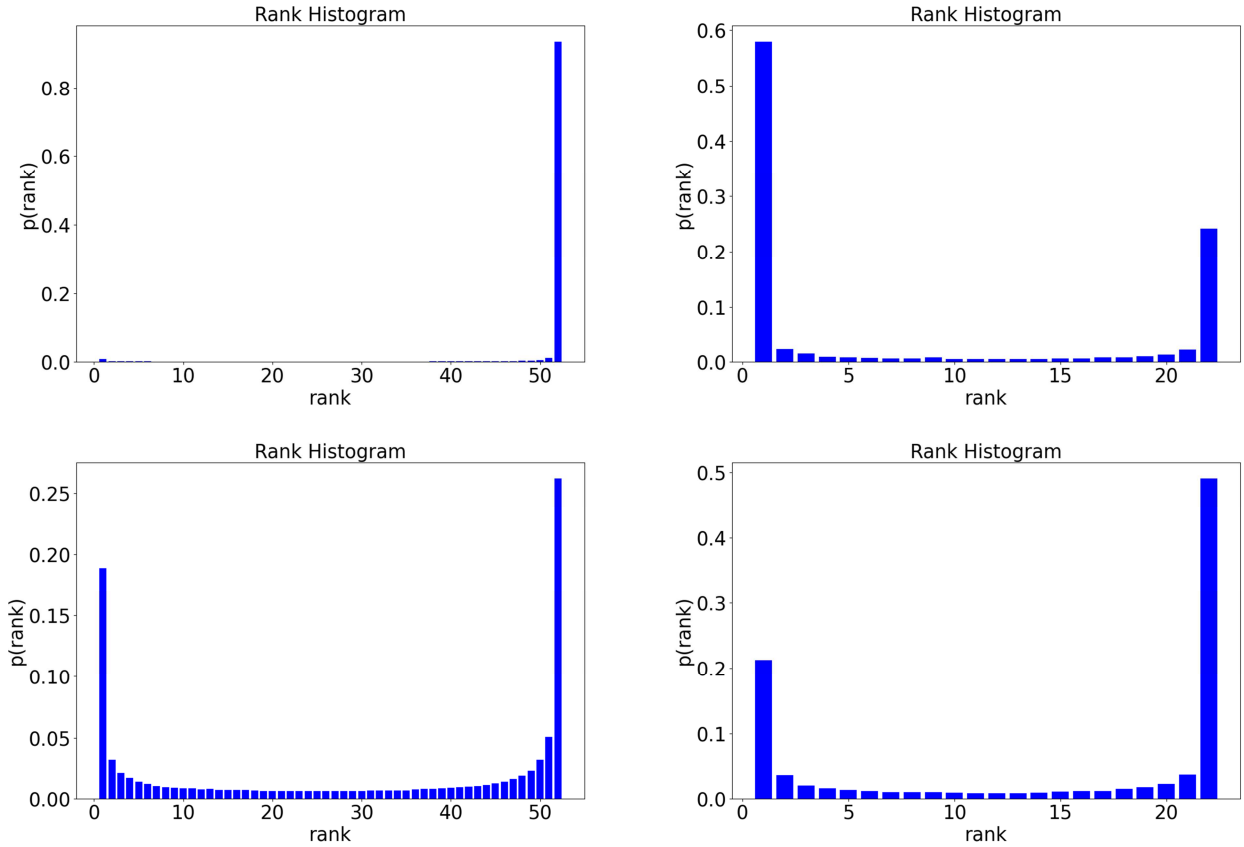

Figure 6. *Rank histograms of 10 to 13 hour wind forecast of raw ECMWF EPS (top right), raw NCEP GEFS (top left), WRF EPS (bottom left), and WRF GEFS (bottom right) for 4 wind farms.*

3.2. Sea Method Evaluation

The proposed SEA method has one hyper-parameter N, the number of ensemble members selected for calculating the ensemble average. The effect of differences in N on forecast performance is presented in Figure 7. Figure 7 shows that the RMSE of raw EPS and raw GEFS increases with increasing value of N while the RMSE of WRF EPS and WRF GEFS decreases first and then increases with a local minimum N of either 2 or 3. Therefore, we choose N = 1 for raw EPS and raw GEFS and N = 2 for WRF EPS and WRF GEFS. The optimal value of N depends on the ensemble type, forecast horizon, and location of wind farms. Similar comparisons are needed when using the SEA method for a different case.

Table 3 summarizes ultra-short-term forecast RMSE comparisons using three ensemble averaging methods: SEA, SEA_Qi, and the ensemble mean of all the ensemble members. The comparisons demonstrate that the SEA method achieves the lowest RMSE among the three methods for all the ensemble forecasts except for WRF EPS and GEFS at farm 4 where the SEA_Qi is the most accurate. The overall most accurate forecast is also the SEA of WRF EPS (2.34 m/s).

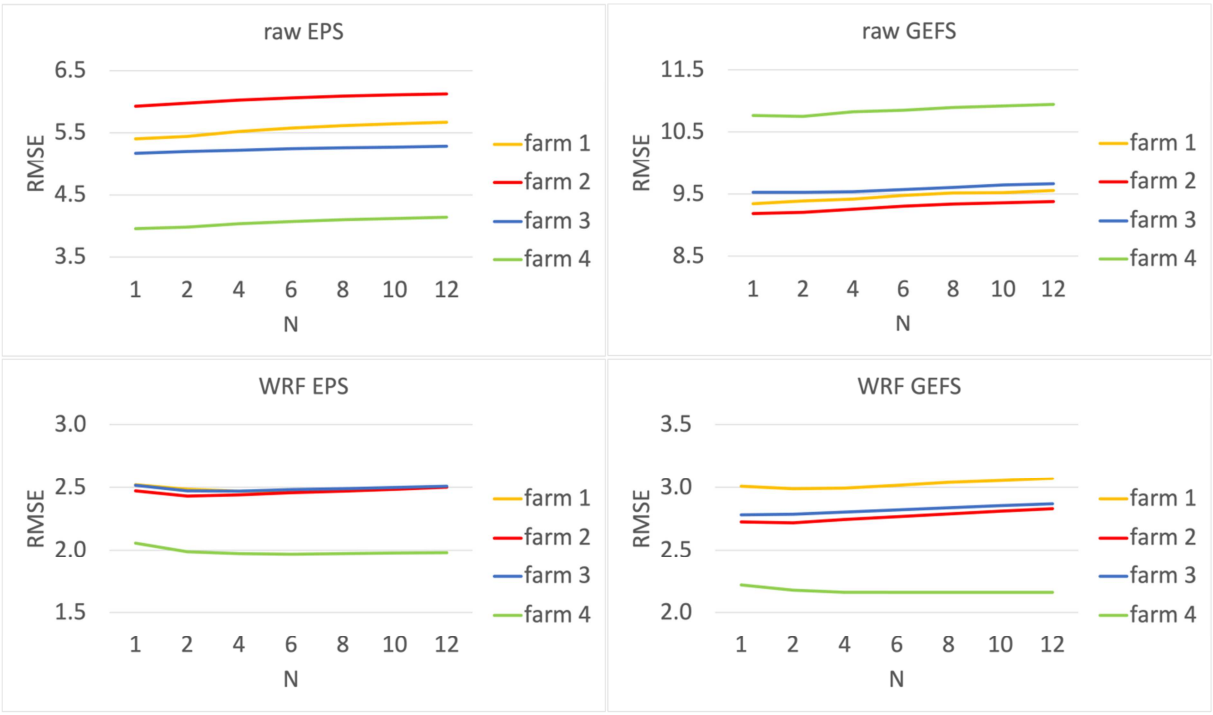

Figure 7. *RMSE of 10 to 13 hour wind forecast of SEA for raw ECMWF EPS (top right), raw NCEP GEFS (top left), WRF EPS (bottom left), and WRF GEFS (bottom right) in 4 wind farms as a function of N from 1 to 12 (see Section 2.2).*

Table 3. *Summary of 10 to 13 hours wind speed forecast RMSE comparisons using three ensemble average methods: SEA with N = 1 for raw EPS and GEFS and 2 for WRF EPS and GEFS (see Section 3.2), SEA_Qi, and ensemble mean of all the members. Bold font indicates the lowest RMSE within each type of ensemble forecast, and italic font indicates the lowest RMSE among all the ensemble forecasts.*

	raw EPS			**raw GEFS**			**WRF EPS**			**WRF GEFS**		
	SEA	**SEA_Qi**	**mean**	**SEA**	**SEA_Qi**	**mean**	**SEA**	**SEA_Qi**	**mean**	**SEA**	**SEA_Qi**	**mean**
	(N=1)			**(N=1)**			**(N=2)**			**(N=2)**		
farm 1	5.40	5.76	5.90	9.35	9.53	9.70	2.49	2.55	2.66	2.99	3.05	3.14
farm 2	5.92	6.17	6.26	9.19	9.37	9.51	2.43	2.59	2.74	2.73	2.80	2.89
farm 3	5.17	5.34	5.42	9.53	9.65	9.80	2.45	2.52	2.61	2.79	2.85	2.92
farm 4	3.97	4.23	4.34	10.76	10.94	11.08	2.01	2.01	2.06	2.18	2.16	2.19
average	5.12	5.37	5.48	9.71	9.87	10.02	2.34	2.42	2.52	2.67	2.71	2.79

4. Conclusion

In this paper, we applied the WRF model to downscale two global ensemble forecast systems, ECMWF EPS and NCEP GEFS. We investigated the added values of downscaling on wind forecast performance for four wind farms over complex terrain in the Sichuan and Yunan provinces of China. The entire year of 2020 forecast data was used for evaluation. The results demonstrate that the ensemble average of the WRF downscaled forecasts has significantly lower RMSE than the raw ensemble forecast for both day-ahead (2.60 and 2.74 m/s of WRF EPS and WRF GEFS compared to 5.26 and 10.13 m/s of raw EPS and raw GEFS) and ultra-short term forecast (2.60 and 2.86 m/s for WRF EPS and WRF GEFS compared to 5.72 and 9.89 m/s of raw EPS and raw GEFS). Thus,

downscaling is quite valuable in improving wind forecast capability in complex terrain, and WRF EPS is more accurate than WRF GEFS.

In addition, we also proposed the SEA method to select N top-performing ensemble members for calculating the ensemble average. The sensitivity tests of ultra-short term forecast performance of the SEA method to changes in N were conducted. Tests showed that the optimal value of N varies for different ensemble forecasts and locations. The SEA method with an optimal value of N also was compared with the ensemble mean of all the ensemble members and the SEA_Qi method. The SEA method showed the best forecast performance (2.34 m/s compared to 2.42 and 2.52 m/s RMSE for WRF EPS).

Future work could consider applying machine learning models using ensemble-related statistics as input features to reduce forecast biases further. Additionally, as the WRF downscaling of all the global ensemble forecast members is very computationally expensive, other methods to build regional EPS should be considered.

Funding

This research was funded by Envision Group Pte. Ltd. and State Grid Gansu Electric Power Company.

Conflict of Interest

The authors declare no conflict of interest.

Acknowledgments

The authors acknowledge Envision Group Pte. Ltd. and State Grid Gansu Electric Power Company for funding the research (Renewable Power Generation Security Study and Application, Grant/Award Number: 522722220025), the European Centre for Medium-Range Weather Forecasts for the data used to drive the WRF model, and the Huawei cloud where the simulations were run.

References

[1] Q. Tu, R. Betz, J. Mo, Y. Fan, Y. Liu, Achieving grid parity of wind power in China – Present levelized cost of electricity and future evolution, Applied Energy. 250 (2019) 1053–1064. https://doi.org/10.1016/j.apenergy.2019.05.039.

[2] X. Xu, D. Niu, B. Xiao, X. Guo, L. Zhang, K. Wang, Policy analysis for grid parity of wind power generation in China, Energy Policy. 138 (2020) 111225. https://doi.org/10.1016/j.enpol.2019.111225.

[3] J. Zhao, Y. Guo, X. Xiao, J. Wang, D. Chi, Z. Guo, Multi-step wind speed and power forecasts based on a WRF simulation and an optimized association method, Applied Energy. 197 (2017) 183–202. https://doi.org/10.1016/j.apenergy.2017.04.017.

[4] M. Marquis, J. Wilczak, M. Ahlstrom, J. Sharp, A. Stern, J. C. Smith, S. Calvert, Forecasting the Wind to Reach Significant Penetration Levels of Wind Energy, Bulletin of the American Meteorological Society. 92 (2011) 1159–1171. https://doi.org/10.1175/2011BAMS3033.1.

[5] A. M. Foley, P. G. Leahy, A. Marvuglia, E. J. McKeogh, Current methods and advances in forecasting of wind power generation, Renewable Energy. 37 (2012) 1–8. https://doi.org/10.1016/j.renene.2011.05.033.

[6] W. Y. Y. Cheng, Y. Liu, A. J. Bourgeois, Y. Wu, S. E. Haupt, Short-term wind forecast of a data assimilation/weather forecasting system with wind turbine anemometer measurement assimilation, Renewable Energy. 107 (2017) 340–351. https://doi.org/10.1016/j.renene.2017.02.014.

[7] J. B. Olson, J. S. Kenyon, I. Djalalova, L. Bianco, D. D. Turner, Y. Pichugina, A. Choukulkar, M. D. Toy, J. M. Brown, W. M. Angevine, E. Akish, J.-W. Bao, P. Jimenez, B. Kosovic, K. A. Lundquist, C. Draxl, J. K. Lundquist, J. McCaa, K. McCaffrey, K. Lantz, C. Long, J. Wilczak, R. Banta, M. Marquis, S. Redfern, L. K. Berg, W. Shaw, J. Cline, Improving Wind Energy Forecasting through Numerical Weather Prediction Model Development, Bulletin of the American Meteorological Society. 100 (2019) 2201–2220. https://doi.org/10.1175/BAMS-D-18-0040.1.

[8] E. N. Lorenz, A study of the predictability of a 28-variable atmospheric model, Tellus. 17 (1965) 321–333. https://doi.org/10.3402/tellusa.v17i3.9076.

[9] Wind Power Density Forecasting Using Ensemble Predictions and Time Series Models, (n.d.). https://ieeexplore.ieee.org/abstract/document/5224014/ (accessed September 11, 2023).

[10] W. J. Shaw, L. K. Berg, J. Cline, C. Draxl, I. Djalalova, E. P. Grimit, J. K. Lundquist, M. Marquis, J. McCaa, J. B. Olson, C. Sivaraman, J. Sharp, J. M. Wilczak, The Second Wind Forecast Improvement Project (WFIP2): General Overview, Bulletin of the American Meteorological Society. 100 (2019) 1687–1699. https://doi.org/10.1175/BAMS-D-18-0036.1.

[11] Z. Pu, E. Kalnay, Numerical Weather Prediction Basics: Models, Numerical Methods, and Data Assimilation, in: Q. Duan, F. Pappenberger, J. Thielen, A. Wood, H. L. Cloke, J. C. Schaake (Eds.), Handbook of Hydrometeorological Ensemble Forecasting, Springer, Berlin, Heidelberg, 2018: pp. 1–31. https://doi.org/10.1007/978-3-642-40457-3_11-1.

[12] T. Palmer, The primacy of doubt: Evolution of numerical weather prediction from determinism to probability, Journal of Advances in Modeling Earth Systems. 9 (2017) 730–734. https://doi.org/10.1002/2017MS000999.

[13] R. Buizza, T. N. Palmer, The Singular-Vector Structure of the Atmospheric Global Circulation, J. Atmos. Sci. 52 (1995) 1434–1456. https://doi.org/10.1175/1520-0469(1995)052<1434:TSVSOT>2.0.CO;2.

[14] F. Molteni, R. Buizza, T. N. Palmer, T. Petroliagis, The ECMWF Ensemble Prediction System: Methodology and validation, Quarterly Journal of the Royal Meteorological Society. 122 (1996) 73–119. https://doi.org/10.1002/qj.49712252905.

[15] Z. Toth, E. Kalnay, Ensemble Forecasting at NMC: The Generation of Perturbations, Bulletin of the American Meteorological Society. 74 (1993) 2317–2330. https://doi.org/10.1175/1520-0477(1993)074<2317:EFANTG>2.0.CO;2.

[16] Z. Toth, E. Kalnay, Ensemble Forecasting at NCEP and the Breeding Method, Monthly Weather Review. 125 (1997) 3297–3319. https://doi.org/10.1175/1520-0493(1997)125<3297:EFANAT>2.0.CO;2.

[17] R. Buizza, P. L. Houtekamer, G. Pellerin, Z. Toth, Y. Zhu, M. Wei, A Comparison of the ECMWF, MSC, and NCEP Global Ensemble Prediction Systems, Monthly Weather Review. 133 (2005) 1076–1097. https://doi.org/10.1175/MWR2905.1.

[18] L. Magnusson, J.-R. Bidlot, M. Bonavita, A. R. Brown, P. A. Browne, G. D. Chiara, M. Dahoui, S. T. K. Lang, T. McNally, K. S. Mogensen, F. Pappenberger, F. Prates, F. Rabier, D. S. Richardson, F. Vitart, S. Malardel, ECMWF Activities for Improved Hurricane Forecasts, Bulletin of the American Meteorological Society. 100 (2019) 445–458. https://doi.org/10.1175/BAMS-D-18-0044.1.

[19] X. Zhou, Y. Zhu, D. Hou, Y. Luo, J. Peng, R. Wobus, Performance of the New NCEP Global Ensemble Forecast System in a Parallel Experiment, Weather and Forecasting. 32 (2017) 1989–2004. https://doi.org/10.1175/WAF-D-17-0023.1.

[20] K. Horvath, A. Bajić, S. Ivatek-Šahdan, Dynamical Downscaling of Wind Speed in Complex Terrain Prone To Bora-Type Flows, Journal of Applied Meteorology and Climatology. 50 (2011) 1676–1691. https://doi.org/10.1175/2011JAMC2638.1.

[21] N. Marjanovic, S. Wharton, F. K. Chow, Investigation of model parameters for high-resolution wind energy forecasting: Case studies over simple and complex terrain, Journal of Wind Engineering and Industrial Aerodynamics. 134 (2014) 10–24. https://doi.org/10.1016/j.jweia.2014.08.007.

[22] P. A. Jiménez, J. Dudhia, Improving the Representation of Resolved and Unresolved Topographic Effects on Surface Wind in the WRF Model, Journal of Applied Meteorology and Climatology. 51 (2012) 300–316. https://doi.org/10.1175/JAMC-D-11-084.1.

[23] F. Weidle, Y. Wang, G. Smet, On the Impact of the Choice of Global Ensemble in Forcing a Regional Ensemble System, Weather and Forecasting. 31 (2016) 515–530. https://doi.org/10.1175/WAF-D-15-0102.1.

[24] Č. Branković, B. Matjačić, S. Ivatek-Šahdan, R. Buizza, Downscaling of ECMWF Ensemble Forecasts for Cases of Severe Weather: Ensemble Statistics and Cluster Analysis, Monthly Weather Review. 136 (2008) 3323–3342. https://doi.org/10.1175/2008MWR2322.1.

[25] H. Zhang, M. Chen, S. Fan, Study on the Construction of Initial Condition Perturbations for the Regional Ensemble Prediction System of North China, Atmosphere. 10 (2019) 87. https://doi.org/10.3390/atmos10020087.

[26] P. A. Jiménez, J. F. González-Rouco, E. García-Bustamante, J. Navarro, J. P. Montávez, J. V.-G. de Arellano, J. Dudhia, A. Muñoz-Roldan, Surface Wind Regionalization over Complex Terrain: Evaluation and Analysis of a High-Resolution WRF Simulation, Journal of Applied Meteorology and Climatology. 49 (2010) 268–287. https://doi.org/10.1175/2009JAMC2175.1.

[27] P. A. Jiménez, J. Dudhia, On the Ability of the WRF Model to Reproduce the Surface Wind Direction over Complex Terrain, Journal of Applied Meteorology and Climatology. 52 (2013) 1610–1617. https://doi.org/10.1175/JAMC-D-12-0266.1.

[28] J. Stanger, I. Finney, A. Weisheimer, T. Palmer, Optimising the use of ensemble information in numerical weather forecasts of wind power generation, Environ. Res. Lett. 14 (2019) 124086. https://doi.org/10.1088/1748-9326/ab5e54.

[29] L. Qi, H. Yu, P. Chen, Selective ensemble-mean technique for tropical cyclone track forecast by using ensemble prediction systems, Quarterly Journal of the Royal Meteorological Society. 140 (2014) 805–813. https://doi.org/10.1002/qj.2196.

[30] R. Kikuchi, T. Misaka, S. Obayashi, H. Inokuchi, H. Oikawa, A. Misumi, Nowcasting algorithm for wind fields using ensemble forecasting and aircraft flight data, Meteorological Applications. 25 (2018) 365–375. https://doi.org/10.1002/met.1704.

[31] R. Huva, G. Song, X. Zhong, Y. Zhao, Comprehensive physics testing and adaptive weather research and forecasting physics for day-ahead solar forecasting, Meteorological Applications. 28 (2021) e2017. https://doi.org/10.1002/met.2017.

[32] S.-Y. Hong, Hongandlim-JKMS-2006, Journal of the Korean Meteorological Society. 42 (2006) 129–151.

[33] S.-Y. Hong, H.-L. Pan, Nonlocal Boundary Layer Vertical Diffusion in a Medium-Range Forecast Model, Monthly Weather Review. 124 (1996) 2322–2339. https://doi.org/10.1175/1520-0493(1996)124<2322:NBLVDI>2.0.CO;2

[34] J. E. Pleim, A. Xiu, Development and Testing of a Surface Flux and Planetary Boundary Layer Model for Application in Mesoscale Models, Journal of Applied Meteorology (1988-2005). 34 (1995) 16–32.

[35] A. Xiu, J. Pleim, Development of a Land Surface Model. Part I: Application in a Mesoscale Meteorological Model, Journal of Applied Meteorology - J APPL METEOROL. 40 (2001) 192–209. https://doi.org/10.1175/1520-0450(2001)040<0192:DOALSM>2.0.CO;2.

[36] J. S. Kain, The Kain–Fritsch Convective Parameterization: An Update, Journal of Applied Meteorology and Climatology. 43 (2004) 170–181. https://doi.org/10.1175/1520-0450(2004)043<0170:TKCPAU>2.0.CO;2.

[37] M.-D. Chou, M. J. Suarez, A Solar Radiation Parameterization for Atmospheric Studies, 1999. https://ntrs.nasa.gov/citations/19990060930 (accessed September 8, 2023).

[38] H. Hersbach, Decomposition of the Continuous Ranked Probability Score for Ensemble Prediction Systems, Weather and Forecasting. 15 (2000) 559–570. https://doi.org/10.1175/1520-0434(2000)015<0559:DOTCRP>2.0.CO;2.

[39] J. M. Sloughter, T. Gneiting, A. E. Raftery, Probabilistic Wind Speed Forecasting Using Ensembles and Bayesian Model Averaging, Journal of the American Statistical Association. 105 (2010) 25–35.

[40] T. M. Hamill, Interpretation of Rank Histograms for Verifying Ensemble Forecasts, Monthly Weather Review. 129 (2001) 550–560. https://doi.org/10.1175/1520-0493(2001)129<0550:IORHFV>2.0.CO;2

[41] D. S. Wilks, Statistical methods in the atmospheric sciences, Academic Press. (2011).